Multi-Cavity Optoelectronic Oscillation Based on a Dispersion-Diversity Heterogeneous Multicore Fibre

Sergi García, Ivana Gasulla

ITEAM Research Institute, Universitat Politècnica de València, Valencia, Spain, sergarc3@iteam.upv.es

Abstract *To the best of our knowledge, we report the first experimental demonstration of tuneable 2-, 3- and 4-cavity optoelectronic oscillation (at radiofrequencies between 7 and 8 GHz) based on exploiting the Vernier effect in a 5-km dispersion-diversity heterogeneous multicore fibre. ©2023 The Authors*

Introduction

The development of multicore fibres (MCFs) has been driven by the need for ultra-high-capacity communications that could take advantage of the space dimension, [1]. By incorporating the chromatic dispersion dimension, MCFs can offer interesting benefits for optical and microwave signal processing, provided that each core is customized to enable tuneable sampled true-time delay line (TTDL) operation, [2]. Within the area of dispersion-managed microwave signal processing, we have previously demonstrated reconfigurable signal filtering [3], radio beam-steering in phased array antennas [4], instantaneous frequency measurement [5], arbitrary waveform generation [6], and multi-gigabit analogue-to-digital conversion [7].

Optoelectronic oscillators (OEOs) are essential devices that find application in a large number of scenarios thanks to their capability to generate ultra-high spectral purity microwave signals, [8]. Multi-cavity Vernier OEOs were developed to improve the oscillating mode spectral purity without compromising the spectral separation between adjacent oscillating modes, [9]. We have previously proposed the exploitation of MCFs to implement multi-cavity OEOs, [10], and we demonstrated non-tuneable OEO on a homogeneous MCF, [11].

To the best of our knowledge, we present in this paper the first experimental demonstration of tuneable multi-cavity optoelectronic oscillation on a dispersion-diversity heterogeneous MCF.

Operation principle

Fig. 1 shows the experimental setup for the proposed multi-cavity Vernier OEO architecture. Its operation principle consists of creating a recirculating feedback loop through a set of optical cavities with slightly different cavity time delays to generate spectrally pure RF oscillation tones at the frequencies given by the inverse of the differential time delay between cavities. For the oscillations to start from noise, the overall system gain must equal 1. The multiple cavities are created by different cores of a 5-km long heterogeneous 7-core MCF. More specifically, the optical signal generated by a tunable laser is modulated by the incoming feedback electrical loop, optically amplified, and injected into four of the fibre cores. At the fibre output, each core signal is equalized in amplitude by a set of variable optical attenuators (VOAs) and photodetected independently. Then, all the cavities are combined, amplified and filtered in the electrical domain. The resulting electrical signal is then injected into the modulator to close the feedback loop. The oscillation spectra is captured in the electrical/optical domains by means of electrical/optical spectrum analyzers.

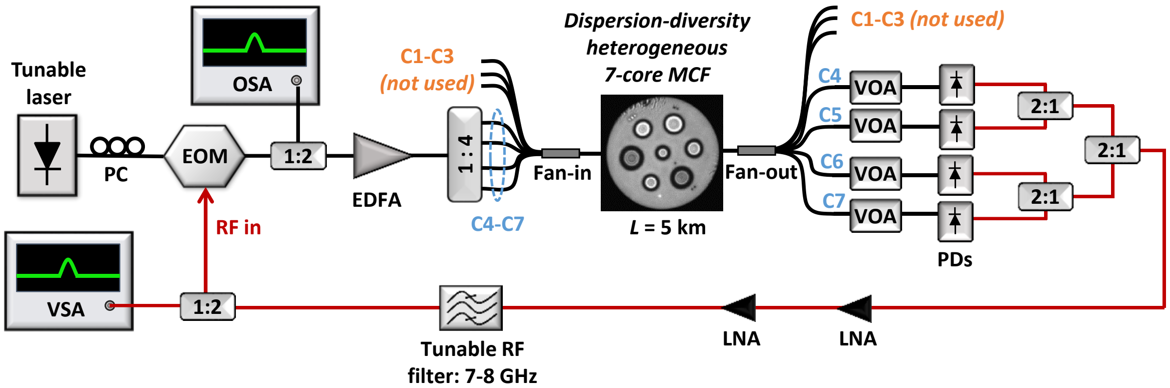

Fig. 1: Experimental setup for the multi-cavity OEO based on a dispersion-diversity heterogeneous MCF. PC: Polarization controller; EOM: Electro-optic modulator; OSA: Optical signal analyser; EDFA: Erbium doped fibre amplifier; VOA: Variable optical attenuator; PD: Photodetector; LNA: Low noise amplifier; VSA: Vector signal analyser; RF: Radiofrequency.

The multi-cavity hosting medium is a custom fabricated dispersion-diversity heterogeneous MCF. The fibre length is L = 5 km and it comprises seven different trench-assisted step-index cores placed in a hexagonal disposition. Each core refractive index profile was tailored independently to satisfy tuneable sampled TTDL operation, [3]. We use cores 4 up to 7, whose measured chromatic dispersions are, respectively, 17.3 up to 20.3 ps/km/nm with an incremental dispersion of ΔD = 1 ps/km/nm, and share a common group delay at the anchor wavelength λ_0 = 1530 nm. At each optical wavelength λ, the cavity differential time delay is given by

$$\Delta\tau(\lambda)=\Delta D\cdot(\lambda-\lambda_0)\cdot L\,, \qquad (1)$$

and thus the oscillation frequencies are, [10],

$$f_o=\frac{n}{\Delta\tau}\,, \qquad (2)$$

for n integer, with a free spectral range FSR = $1/\Delta\tau$. Fig. 2 (a) depicts the measured mean core differential group delays, $\Delta\tau$, as a function of the optical wavelength for cores 4 up to 7. By substituting these $\Delta\tau$ values into Eq. (2), we see that the oscillation frequencies can then be continuously tuned in the microwave band by sweeping the laser operation optical wavelength in the C band.

Results

We have implemented three different multi-cavity OEO configurations: A 2-cavity OEO by using cores 4 and 5; a 3-cavity OEO by using cores 4, 5 and 6; and a 4-cavity OEO with cores 4 up to 7. The cavity differential time delay, $\Delta\tau$, is practically identical in all three cases, and so they are the frequencies of oscillation.

The uneven signal level at the different RF frequencies, mainly caused by frequency-dependent RF components (such as RF cables and couplers) and the inherent behaviour of the electro-optical modulator, made it impossible to achieve tuneable free-running oscillations. Fig. 2 (b) illustrates the measured system transfer function at the optical wavelength of 1555 nm for the 2- (blue), 3- (orange), and 4-cavity (yellow) configurations. As lower frequencies have much higher RF power, the OEO will tend to oscillate there. Thus, an RF filter was necessary to reject the lower frequency band and allow oscillation frequency reconfigurability. We use a tuneable RF filter between 7 and 8 GHz with a -3-dB bandwidth of BW_{-3dB} = 30 MHz. For each operation optical wavelength, the filter central frequency is then adequately tuned to capture the corresponding oscillating frequency.

Fig. 3 (a) depicts the oscillation frequencies

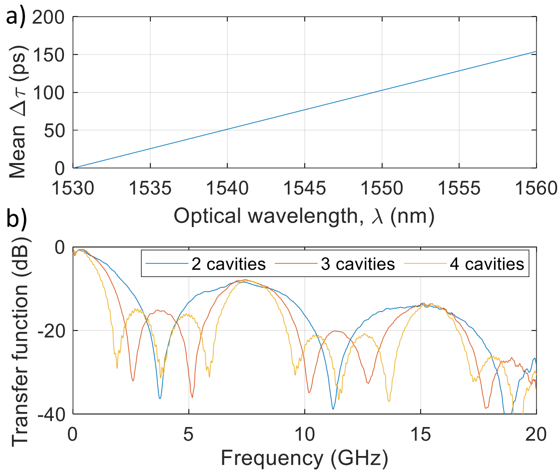

Fig. 2: (a) Mean of the measured core differential group delay, $\Delta\tau$, for cores 4 up to 7 with the optical wavelength. (b) Measured multi-cavity OEO transfer function.

for the 4-cavity configuration at three different optical wavelengths. Blue, orange, and yellow lines represent, respectively, the measured oscillation spectra at the optical wavelengths of 1555.6, 1556.5 and 1557.8 nm. At each optical wavelength, the core differential group delays are 128, 133 and 139 ps, respectively for λ = 1555.6, 1556.5 and 1557.8 nm, resulting in oscillation frequencies located at 7.8, 7.5 and 7.2 GHz, respectively. Fig. 3 (b) shows the relationship between the oscillation frequency and the operation optical wavelength (black dotted line).

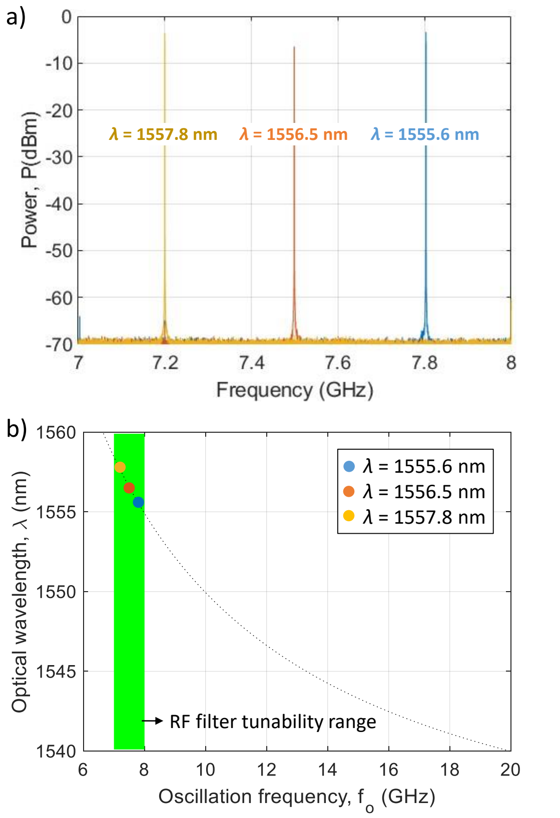

Fig. 3: (a) Measured oscillation tone power for three different optical wavelengths. (b) Relationship between the oscillation frequency and the operation optical wavelength.

Filled circles correspond to the measured oscillation frequencies of Fig. 3(a), while the green-filled rectangle represents the frequency tunability range of the RF filter. As shown, the oscillation frequency tunability is restricted by the RF filter frequency tunability range. Different RF filters, such as a basic low-pass filter with a cut-off frequency of 5 GHz would bring a wider frequency reconfigurability range, allowing continuous OEO oscillation frequency tunability between 6 and 20 GHz by sweeping the optical wavelength between 1540 and 1560 nm.

Fig. 4 compares the oscillation spectrum of the oscillating tone at 7.8 GHz for the 2-cavity (blue), 3-cavity (orange) and 4-cavity (yellow) OEOs in a 200-MHz bandwidth around the oscillating mode. The inset shows a zoomed 2-MHz bandwidth around the oscillation peak. We see a single-frequency spectrally pure oscillation with an important reduction in the single-cavity spurious tones, whose FSR is ≈ 40 kHz (single cavity of 5 km) due to the multi-cavity configuration. Similar results are obtained with all three configurations, with a slight reduction in the single-cavity spurious tones as the number of cavities increases. In addition, the frequency stability of the oscillation mode improves as the number of cavities increases, considerably reducing possible frequency hopping caused by the inevitable cavity delay variations due to environmental effects. We should note that the RF filter bandwidth (30 MHz) is much higher than the FSR of the single-cavity oscillating modes (≈40 kHz), so that the oscillating frequency selection is performed by the multi-cavity configuration itself, further alleviating the RF filter bandwidth requirements.

Finally, we measured the phase noise spectrum of all three configurations by means of a Keysight Infiniium real-time oscilloscope (UXR0704AP) and the PathWave Vector Signal Analysis (89600 VSA) software module. Fig. 5

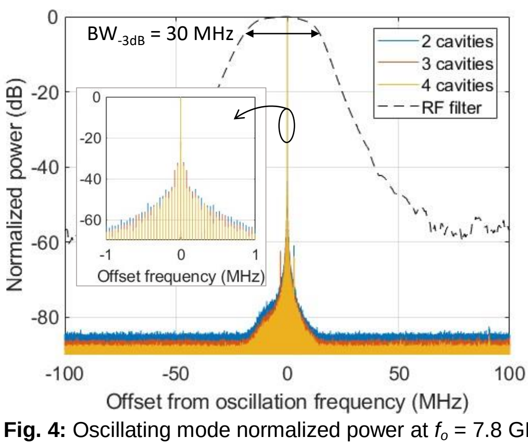

Fig. 4: Oscillating mode normalized power at f_o = 7.8 GHz for the multi-cavity OEO when the laser operates at the optical wavelength of 1555.6 nm. Inset: 2-MHz zoom.

shows the measured phase noise spectrum for the 2-cavity (blue), 3-cavity (orange) and 4-cavity (yellow) OEOs from 10 Hz up to 10 MHz frequency offset from the oscillating frequency f_o = 7.8 GHz (at the optical wavelength of 1555.6 nm). At 1-kHz offset, the phase noise is -120 dBc/Hz, decreasing down to -150 dBc/Hz at a 100-kHz offset, which are in the order of the current best-case OEOs reported in the literature, [9,12]. The single-cavity spurious peaks are further suppressed, with a maximum value below -75 dBc/Hz for the closest peak (at ≈40 kHz offset) without the need of a selective RF filter bandwidth. Comparing all three configurations, we observe again that increasing the number of cavities tends to produce a slight reduction on the single-cavity spurious peaks.

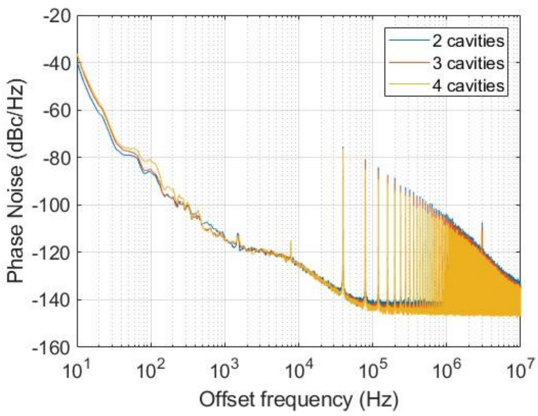

Fig. 5: Measured phase noise spectra for the multi-cavity OEO oscillation frequency f_o = 7.8 GHz when the laser operates at the optical wavelength of 1555.6 nm.

Conclusions

We have reported the first-ever experimental demonstration of multi-cavity OEO on a dispersion-diversity MCF by exploiting the Vernier effect. The multi-cavity medium is a 5-km heterogeneous 7-core fibre that behaves as a sampled TTDL. We successfully demonstrated tuneable 2-, 3- and 4-cavity OEOs at the RF frequencies between 7 and 8 GHz. The measured phase noise is -120 dBc/Hz at 1-kHz offset and decreases to -150 dBc/Hz at 100 kHz. A major advantage of this approach is that it provides higher time delay stability than other parallel architectures, since all cavities are hosted in a single fibre and thus subjected to identical environmental conditions. Increasing the number of cavities improves the frequency stability, reducing undesired frequency hopping.

Acknowledgements

ERC Consolidator Grant 724663, the Spanish Ministerio de Ciencia e Innovación Grant PID2020-118310RB-100, and Universitat Politècnica de València PAID-PD-22 grant and PAID-10-21 fellowship for S. García.

References

[1] D. Richardson, J. Fini, and L. Nelson, “Space-division multiplexing in optical fibres,” *Nature Photonics*, vol. 7, pp. 354–362, 2013, DOI: 10.1038/nphoton.2013.94

[2] I. Gasulla and J. Capmany, "Microwave Photonics Applications of Multicore Fibers," in *IEEE Photonics Journal*, vol. 4, no. 3, pp. 877-888, 2012, DOI: 10.1109/JPHOT.2012.2199101

[3] S. García, M. Ureña, and I. Gasulla, “Dispersion-diversity multicore fiber signal processing”, *ACS Photonics*, vol. 9, pp. 2850–2859, 2022, DOI: 10.1021/acsphotonics.2c00910

[4] M. Ureña, S. García, J. I. Herranz, and I. Gasulla, “Experimental demonstration of dispersion-diversity multicore fiber optical beamforming,” *Optics Express*, vol. 30, no. 18, pp. 32783-32790, 2022, DOI: 10.1364/OE.468436

[5] E. Nazemosadat, S. García, and I. Gasulla, "Heterogeneous multicore fiber-based microwave frequency measurement," Optics Express, vol. 30, no. 15, pp. 26886-26895, 2022, DOI: 10.1364/OE.463152

[6] M. Ureña, S. García, and I. Gasulla, "Ultra-Wideband Pulse Generation Based on Dispersion-Diversity Multicore Fiber," in *Optical Fiber Communication Conference (OFC) 2023*, San Diego, United States, 2023, paper M1J.1.

[7] S. García, M. Ureña and I. Gasulla, "Photonic-Assisted Analog-to-Digital Conversion Based on a Dispersion-Diversity Multicore Fiber," in *IEEE Journal of Selected Topics in Quantum Electronics*, vol. 29, no. 6: Photonic Signal Processing, pp. 1-8, 2023, DOI: 10.1109/JSTQE.2023.3267507

[8] X. Yao and L. Maleki, "Converting light into spectrally pure microwave oscillation," Optics Letters, vol. 21, no. 7, pp. 483-485, 1996, DOI: 10.1364/OL.21.000483

[9] Z. Tang, S. Pan, D. Zhu, R. Guo, Y. Zhao, M. Pan, D. Ben, and J. Yao, "Tunable Optoelectronic Oscillator Based on a Polarization Modulator and a Chirped FBG," in *IEEE Photonics Technology Letters*, vol. 24, no. 17, pp. 1487-1489, 2012, DOI: 10.1109/LPT.2012.2205235

[10] S. García and I. Gasulla, "Multi-cavity optoelectronic oscillators using multicore fibers," Optics Express, vol. 23, no. 3, pp. 2403-2415, 2015, DOI: 10.1364/OE.23.002403

[11] S. García and I. Gasulla, "Experimental demonstration of multi-cavity optoelectronic oscillation over a multicore fiber," Optics Express, vol. 25, no. 20, pp. 23663-23668, 2017, DOI: 10.1364/OE.25.023663

[12] O. Lelièvre, V. Crozatier, G. Baili, P. Berger, L. Morvan, G. Pillet, D. Dpñfo, O. Llopis, F. Goldfarb, and F. Bretenaker, "Ultra-low-noise optoelectronic oscillator at 10 GHz based on a short fiber delay," in *2016 European Frequency and Time Forum (EFTF)*, York, UK, 2016, pp. 1-2, DOI: 10.1109/EFTF.2016.7477835